



HAL
open science

Beyond-mean-field effects in Rabi-coupled two-component Bose-Einstein condensate

L Lavoine, A Hammond, A Recati, D Petrov, T Bourdel

► **To cite this version:**

L Lavoine, A Hammond, A Recati, D Petrov, T Bourdel. Beyond-mean-field effects in Rabi-coupled two-component Bose-Einstein condensate. 2021. hal-03232484v1

HAL Id: hal-03232484

<https://hal.science/hal-03232484v1>

Preprint submitted on 21 May 2021 (v1), last revised 15 Nov 2021 (v5)

HAL is a multi-disciplinary open access archive for the deposit and dissemination of scientific research documents, whether they are published or not. The documents may come from teaching and research institutions in France or abroad, or from public or private research centers.

L'archive ouverte pluridisciplinaire **HAL**, est destinée au dépôt et à la diffusion de documents scientifiques de niveau recherche, publiés ou non, émanant des établissements d'enseignement et de recherche français ou étrangers, des laboratoires publics ou privés.

Beyond-mean-field effects in Rabi-coupled two-component Bose-Einstein condensate

L. Lavoine,¹ A. Hammond,¹ A. Recati,² D. Petrov,³ and T. Bourdel^{1,*}

¹*Laboratoire Charles Fabry, UMR 8501, Institut d'Optique, CNRS, Université Paris-Saclay, Avenue Augustin Fresnel, 91127 Palaiseau CEDEX, France*

²*INO-CNR BEC Center and Dipartimento di Fisica, Università degli Studi di Trento, 38123 Povo, Italy and Trento Institute for Fundamental Physics and Applications, INFN, 38123 Trento, Italy*

³*Université Paris-Saclay, CNRS, LPTMS, 91405 Orsay, France*

(Dated: May 21, 2021)

We theoretically calculate and experimentally measure the beyond-mean-field (BMF) equation of state in a coherently-coupled two-component Bose-Einstein condensate (BEC) in the regime where averaging of the interspecies and intraspecies coupling constants over the hyperfine composition of the single-particle dressed state predicts the exact cancellation of the two-body interaction. We show that with increasing the Rabi frequency, the BMF energy density crosses over from the nonanalytic Lee-Huang-Yang (LHY) scaling $\propto n^{5/2}$ to an expansion in integer powers of density, where, in addition to a two-body BMF term $\propto n^2$, there emerges a repulsive three-body contribution $\propto n^3$. We work in a Rabi-coupled two-component ³⁹K condensate which is released in a waveguide. Its expansion dynamics is governed by the BMF energy allowing for its quantitative measurement. By studying the expansion with and without Rabi coupling, we reveal an important feature relevant for observing BMF effects and associated phenomena in mixtures with spin-asymmetric losses: Rabi coupling helps preserve the spin composition and thus prevents the system from drifting away from the point of vanishing mean field.

Vacuum effects are among the most striking features of quantum field theories. The high degree of control of cold gases has made these systems ideal candidates to identify and measure the role of quantum fluctuations in matter fields. For instance, using Bose gases, quantum phonons fluctuations [1], phononic Lamb shift [2], dynamical phononic Casimir effect [3], as well as evidence of Hawking-like radiation from analog gravity configurations [4] have been reported.

For a weakly interacting Bose gas quantum fluctuations cause the BEC depletion [5, 6] and lead to the so-called LHY correction to the mean-field (MF) equation of state [7]. This BMF correction has found experimental verification a few years ago [8, 9]. More recently, self-trapped quantum droplets were stabilized against collapse by BMF effects in single component dipolar BECs [10, 11] and in two-component BEC mixtures [12–14]. In the latter case, the MF interaction is greatly reduced by the compensation between intraspecies repulsion and interspecies attraction while the BMF energy originating from quantum fluctuations remains finite.

In this Letter we consider a Bose gas formed by atoms with two internal levels, which are coherently coupled [15]. The BEC order parameter is then a two-component vector and the relative phase excitations are gapped due to the coherent drive. Such systems have been thoroughly analyzed on the MF level and used in variety of experiments on coherent Rabi oscillations [16, 17], internal self-trapping effects [18], ferromagnetic classical bifurcation [19], Kibble-Zurek mechanism [20], control of the two-body interaction [21–23], and magnetic domain wall dynamics [24]. For sufficiently attractive interspecies interaction such Rabi-coupled BECs are predicted to sustain droplets in the symmetric case, where the Rabi coupling

is resonant and the intraspecies coupling constants are equal to each other. The stabilization mechanism is interpreted from the few-body perspective as an emergent three-body repulsion [22] or as a many-body BMF effect due to a structural change in the excitation spectrum [25].

Here, we analytically calculate the BMF energy density in the experimentally relevant case of an asymmetric Rabi-coupled Bose mixture in the whole range of Rabi frequencies Ω . We show that the BMF correction crosses over from the LHY law $\propto n^{5/2}$ for small Ω to the regular expansion in integer powers of n for large Ω . The quadratic term in the latter limit can be understood as a renormalization of the two-body interaction, the cubic term as an emergent three-body interaction, and so on. Experimentally, we quantitatively measure the BMF energy as a function of Ω by observing the expansion of a condensed ³⁹K spin-mixture in a waveguide at the point of vanishing mean-field [26]. In the absence of Rabi coupling, we observe that asymmetric losses between the two spin states drive the spin composition away from the point of zero MF interaction and thus strongly affect the expansion.

We consider a Bose gas of N atoms possessing two internal states, $\sigma = \uparrow, \downarrow$, coherently coupled with the Rabi frequency Ω and detuning δ . In the rotating wave approximation the Hamiltonian of the mixture reads [15, 27]

$$\hat{H} = \int \left(\sum_{\sigma} -\hat{\Psi}_{\sigma\mathbf{r}}^{\dagger} \frac{\nabla_{\mathbf{r}}^2}{2} \hat{\Psi}_{\sigma\mathbf{r}} + \sum_{\sigma\sigma'} \hat{\Psi}_{\sigma\mathbf{r}}^{\dagger} \xi_{\sigma\sigma'} \hat{\Psi}_{\sigma'\mathbf{r}} + \sum_{\sigma,\sigma'} \frac{g_{\sigma\sigma'}}{2} \hat{\Psi}_{\sigma\mathbf{r}}^{\dagger} \hat{\Psi}_{\sigma'\mathbf{r}}^{\dagger} \hat{\Psi}_{\sigma\mathbf{r}} \hat{\Psi}_{\sigma'\mathbf{r}} \right) d\mathbf{r}, \quad (1)$$

where $\hat{\Psi}_{\sigma r}$ is the annihilation Bose field operator, $\xi = -(\delta\sigma_z + \Omega\sigma_x)/2$ is the single particle spin Hamiltonian written in terms of the Pauli matrices acting in the $|\uparrow\rangle$ - $|\downarrow\rangle$ space, and $g_{\sigma\sigma'} = 4\pi a_{\sigma\sigma'}$ are the coupling constants for the σ - σ' interaction with the scattering lengths $a_{\sigma\sigma'}$. In Eq. (1) and in the rest of the paper we adopt the units $\hbar = m = 1$, where m is the mass of the particles.

Assuming zero-temperature and weak interactions, we follow the usual Bogoliubov procedure by separating the dominant condensate contribution and writing the field operator as $\hat{\Psi}_{\sigma r} = \sqrt{n_\sigma} + \hat{\phi}_{\sigma r}$, where n_σ are the condensate densities and $\hat{\phi}_{\sigma r}$ annihilate particles with nonzero momenta. Neglecting $\hat{\phi}$ and substituting $\hat{\Psi}_{\sigma r} = \sqrt{n_\sigma}$ into Eq. (1) we obtain the MF energy density

$$E_{\text{MF}} = \frac{\delta}{2} \frac{1 - \alpha^2}{1 + \alpha^2} n - \frac{\Omega\alpha}{1 + \alpha^2} n + \frac{g_{\uparrow\uparrow}\alpha^4 + g_{\downarrow\downarrow} + 2g_{\uparrow\downarrow}\alpha^2}{(1 + \alpha^2)^2} \frac{n^2}{2}, \quad (2)$$

where $n = n_\uparrow + n_\downarrow$ and $\alpha = \sqrt{n_\uparrow/n_\downarrow}$. In the limiting case of vanishing density (or interactions), E_{MF} gets minimized for $\alpha = \alpha_0 = \delta/\Omega + \sqrt{1 + \delta^2/\Omega^2}$, consistent with the condensation in the dressed state $|-\rangle = (\alpha_0|\uparrow\rangle + |\downarrow\rangle)/\sqrt{1 + \alpha_0^2}$, which is the ground state of ξ . The coefficient in front of $n^2/2$ in Eq. (2) is then the MF coupling constant corresponding to the scattering length $a_{--} = (a_{\uparrow\uparrow}\alpha_0^4 + a_{\downarrow\downarrow} + 2a_{\uparrow\downarrow}\alpha_0^2)/(1 + \alpha_0^2)^2$ [23]. For $a_{\uparrow\uparrow} > 0$, $a_{\downarrow\downarrow} > 0$, and $a_{\uparrow\downarrow} < 0$, a_{--} exhibits a minimum as a function of δ (or α_0). We are interested in the particular configuration of the scattering lengths (controlled by the magnetic field) and the RF drive parameters where this minimum touches zero. This translates into two conditions:

$$\delta a = 0 \text{ and } \alpha_0 = \beta, \quad (3)$$

where we have introduced the scattering length detuning $\delta a = a_{\uparrow\downarrow} + \sqrt{a_{\uparrow\uparrow}a_{\downarrow\downarrow}}$ and the interaction asymmetry parameter $\beta = (a_{\downarrow\downarrow}/a_{\uparrow\uparrow})^{1/4}$. Note that for finite n the energy E_{MF} , upon minimization with respect to α , is not, in general, a quadratic function of n since the optimal polarization parameter α does depend on n . In particular, the system can feature a three-body attraction already on the MF level [28]. However, the minimum of a_{--} is a special point where both terms on the right-hand side of Eq. (2) are minimized at $\alpha = \alpha_0$ independent of n . At this point E_{MF} is thus quadratic in n . If, in addition, we tune δa to zero [configuration (3)], the minimum of a_{--} also vanishes and the condensate becomes noninteracting on the MF level.

We shall now discuss the influence of BMF effects on the equation of state. In the Bogoliubov approach the leading BMF term is obtained by expanding the Hamiltonian (1) up to quadratic terms in $\hat{\phi}_\sigma$ and by summing the zero point energies of the corresponding Bogoliubov modes. In the symmetric case ($a_{\uparrow\uparrow} = a_{\downarrow\downarrow}$ and $\delta = 0$) the calculation has been performed in Ref. [25]. The general asymmetric case is technically more difficult because of

cumbersome expressions for the Bogoliubov modes [29]. However, under the conditions (3), these expressions simplify and read

$$E_{p,-} = p^2/2, \\ E_{p,+} = \sqrt{(p^2/2 + \tilde{\Omega})(p^2/2 + \tilde{\Omega} - 2g_{\uparrow\downarrow}n)},$$

where p is the momentum and $\tilde{\Omega} = \Omega(\alpha_0 + 1/\alpha_0)/2$. The BMF energy density can then be reduced to the form [29]

$$E_{\text{BMF}} = \frac{8(-g_{\uparrow\downarrow}n)^{5/2}}{15\pi^2} I\left(\frac{\tilde{\Omega}}{-2g_{\uparrow\downarrow}n}\right), \quad (4)$$

$$\text{with } I(y) = \frac{15}{4} \int_0^1 \sqrt{x(1-x)(x+y)} dx.$$

Equation (4) remains a good approximation for the BMF energy density as long as $|\delta a/a_{\uparrow\downarrow}| \ll 1$ and $|\alpha_0 - \beta| \ll 1$. The function $I(y)$ is a monotonically growing function, which tends to 1 for $y = \tilde{\Omega}/(-2g_{\uparrow\downarrow}n) \rightarrow 0$. This is the limit of two uncoupled condensates where Eq. (4) reduces to the LHY form, responsible for the BMF stabilization of quantum droplets in binary mixtures [12]. In the opposite limit $I(y)$ can be expanded in powers of $1/y \ll 1$, the first two leading terms being $I(y) \approx (15\pi/128)(1/\sqrt{y} + 4\sqrt{y})$. The substitution of this expansion into Eq. (4) gives

$$E_{\text{BMF}} \approx \frac{\sqrt{\tilde{\Omega}}}{2\sqrt{2}\pi} g_{\uparrow\downarrow}^2 \frac{n^2}{2} + \frac{3}{4\sqrt{2}\pi\sqrt{\tilde{\Omega}}} |g_{\uparrow\downarrow}|^3 \frac{n^3}{6}, \quad (5)$$

which is qualitatively different from the LHY $n^{5/2}$ scaling. The two terms in Eq. (5) can be interpreted as a BMF-renormalized two-body interaction and an emergent three-body term, respectively. In the symmetric case, the three-body term agrees with the exact three-body calculation [22], if the latter is taken in the regime where the characteristic length scale $1/\sqrt{\tilde{\Omega}}$, associated to the drive, is much larger than $a_{\sigma\sigma'}$. Curiously, the three-body coupling constant $g_3 = 3|g_{\uparrow\downarrow}|^3/(4\pi\sqrt{2}\tilde{\Omega})$ which we have obtained here by using the many-body Bogoliubov approach would be significantly more difficult to calculate in the asymmetric case by using the general three-body formalism of Ref. [22].

We now turn to the experimental measurement of the BMF energy. The latter, in a situation where the MF interaction is cancelled, is directly measured through the released energy in a one-dimensional expansion experiment. We work with the second and third lowest Zeeman states of the lowest manifold of ^{39}K , namely $|\uparrow\rangle = |F = 1, m_F = -1\rangle$ and $|\downarrow\rangle = |F = 1, m_F = 0\rangle$. At a magnetic field of 56.830(1) G, the three relevant scattering lengths are $a_{\uparrow\uparrow} = 33.4 a_0$, $a_{\downarrow\downarrow} = 83.4 a_0$ and $a_{\uparrow\downarrow} = -53.2 a_0$, where a_0 is the atomic Bohr radius [30]. The minimum of a_{--} is then $-0.2 a_0$. We have checked that the corresponding residual MF energy is a small

correction as compared to the BMF energy for our parameters. The experiment starts with a quasi pure BEC in state $|\uparrow\rangle$. The atoms are optically trapped in an elongated harmonic potential with frequencies $(\omega_x, \omega_y, \omega_z) = (137, 137, 25.4)$ Hz.

The coherent mixture in $|-\rangle$ is prepared in an adiabatic passage, in which the radio-frequency (RF) detuning is swept from $\delta = 7.5\Omega$ to its final value $\delta \approx 0.23\Omega$, for which $\alpha_0 \approx \beta$. During the RF sweep, a_{--} decreases from $33.3a_0$ to a value close to 0. Its shape and duration of 9 ms are chosen in order to be adiabatic not only with respect to the internal-state dynamics but also with respect to the radial evolution of the wave function, which progressively shrinks and approaches the ground state of the radial harmonic confinement. We have checked that we cannot detect any residual oscillations of the radial size after the RF sweep. In addition, the axial trap frequency is progressively turned off during the sweep and adjusted such that the gas is neither axially expanding nor shrinking in a three-dimensional expansion after the sweep. The radially confined condensate is then free to expand in the axial direction for a time of 75 ms. During the final stage of the expansion, we sweep back the RF frequency to its initial value to map the states $|-\rangle$ and $|+\rangle$ back onto $|\uparrow\rangle$ and $|\downarrow\rangle$, which we independently detect by fluorescent imaging after a short Stern-Gerlach separation.

Interestingly, we observe that the atoms remain in state $|-\rangle$ [35], which might be surprising as losses are known to take place mostly in state $|\downarrow\rangle$ and thus could lead to the creation of $|+\rangle$. In order to understand the spin dynamics, we can model the losses by adding $-i\Gamma/2$ to the second diagonal term in ξ . Diagonalizing the resulting matrix, we see that for $\Gamma \ll \Omega$ the initial state $|-\rangle$ remains essentially unchanged, except that it decays with the rate $\approx \Gamma \langle -|\downarrow\rangle|^2 = \Gamma/(1 + \alpha_0^2)$. In our experiment Γ is at most $\sim 20\text{s}^{-1}$, which is much lower than Ω . We thus conclude that the spin-dependent loss in our case reduces to an effective loss in the dressed state, with Γ weighted by the fraction of the lossy component.

For each value of the Rabi frequency Ω , we first measure the condensate density profile after expansion as a function of the detuning δ . The condensate sizes are extracted from fits with 1D Thomas-Fermi density profiles $\propto 1 - (z/R_{\text{TF}})^2$ (see Fig. 1). In principle, the condensate expansion is governed by the total energy $E_{\text{MF}} + E_{\text{BMF}}$. However, the variation of the MF energy as a function of δ is much stronger than the corresponding variation of E_{BMF} such that the latter can be approximated by a constant [36]. As a consequence, the variation of our measured size is dominated by the variation of a_{--} . As we have explained above, under the conditions (3), the MF term vanishes ($a_{--} \approx 0$) and the expansion of the cloud is governed by the BMF term. In Fig. 2, we plot the measured minimal size as a function of the Rabi frequency $\Omega/2\pi$. For Rabi frequencies $\Omega/2\pi$ between 6 kHz

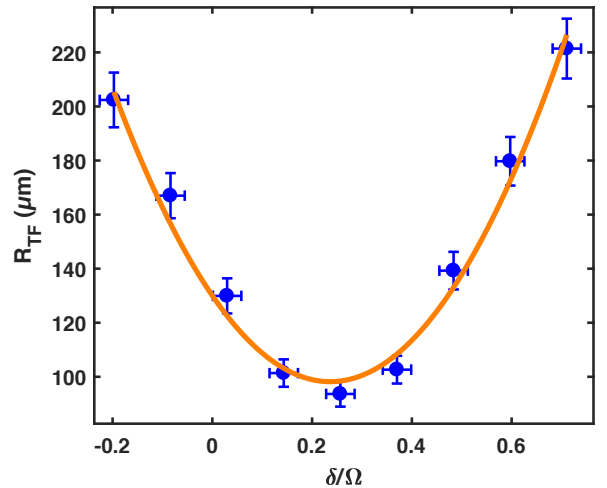


FIG. 1: Experimental Thomas-Fermi radius of the condensate after 75 ms of expansion as a function of δ/Ω , for a Rabi frequency $\Omega/2\pi = 12.29$ kHz. The curve is a parabolic guide to the eye.

and 38 kHz, we observe a slow increase of the measured size as a function of Ω , which corresponds to an increase of the LHY energy as predicted previously. More precisely, the size after a long time of flight is expected to scale with $\sqrt{E_{\text{LHY}}} \propto \Omega^{1/4}$ for a dominant two-body term valid at large Ω , which is indeed close to our observed behavior. At low Rabi frequencies, below 6 kHz, we observe an increase of the size which we attribute to low frequency magnetic field noise. In a 50 μs Ramsey sequence, we have measured a standard deviation of the magnetic field $\Delta B \sim 0.8(2)$ mG corresponding to $\Delta\delta \sim 560$ Hz. This fluctuations leads to an increased average value of the scattering length $\Delta a_{--} \approx 48(\Delta\delta/\Omega)^2 a_0$, which can explain our observed increasing size for low value of Ω [37].

We now precisely model our experiment. In brief, we solve the wave-function evolution through a single component one-dimensional non-linear Schrödinger equation in which we properly account for the BMF energy E_{BMF} [31]. The axial initial wave function is taken to be $\propto 1 - (z/R_{\text{TF}})^2$, such that the axial density profile is the one of the initial 3D Thomas-Fermi condensate before the RF sweep. The spin healing length is smaller than the radial cloud size and the LHY energy is treated in a local density approximation in the radial direction [32]. Since the chemical potential can be of the order of the radial confinement energy ω_{\perp} (especially at large Ω), we take into account, as a function of the 1D density, the correction to the Gaussian radial profile due to the dominant two-body BMF contribution. The 1D energy density is then found by radial integration, and the chemical potential entering the Schrödinger equation by partial derivation with respect to the 1D density. The magnetic field noise can be accounted for by an increase

of a_{--} entering the MF term.

We find that our model quantitatively reproduces our experimental results (see Fig. 2). The initial atom number 1.05×10^5 have been adjusted to match the experimental data and corresponds within 5% to a calibration using the condensation temperature (which precision is $\sim 20\%$). The initial peak density is $n \sim 5 \times 10^{20} \text{ m}^{-3}$. A three-body loss coefficient $K_{---}/3! = 4 \times 10^{-28} \text{ cm}^6 \cdot \text{s}^{-1}$ has been adjusted to match our observed $\sim 30\%$ atom loss during the expansions [38]. As an example, for a value $\Omega/2\pi = 10 \text{ kHz}$, $\tilde{\Omega}/(-2g_{\uparrow\downarrow}n) \approx 1$ and the initial two-body and three-body energies per particle are found to be 20 Hz and 3.2 Hz, respectively.

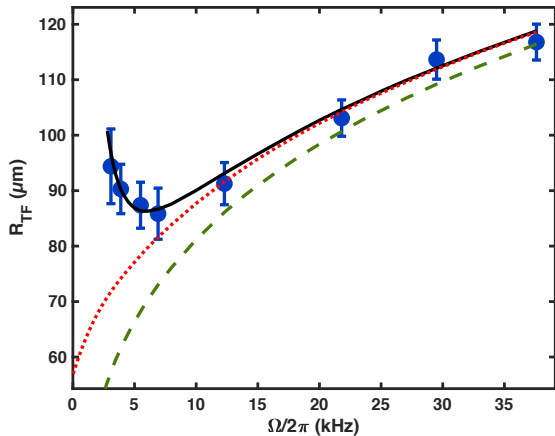


FIG. 2: Thomas-Fermi radius of the condensate after 75 ms of expansion as a function of the Rabi coupling strength. Each point is obtained by averaging 15 fluorescence images and the error bars correspond to the single shot standard deviation. The curves correspond to quasi-1D extended Gross-Pitaevskii simulations (see text). Red dotted curve: BMF description; black solid curve: BMF description with the addition of magnetic field noise; green dashed curve: BMF description restricted to the two-body term.

Finally, we can also repeat the expansion measurement while removing the RF coupling field at the end of the sweep such that we are left with two uncoupled condensates. The losses then dominantly take place in state $|\downarrow\rangle$ and contrary to the coupled case, α quickly deviates from its initial value β . Moreover, we observe after a Stern-Gerlach separation that the two clouds behave differently in the expansion (see Fig. 3). The $|\downarrow\rangle$ condensate does not expand much whereas the $|\uparrow\rangle$ condensate exhibits a double structure with a low energy central part. This behavior is reminiscent of previous observations in droplet configuration where excess $|\uparrow\rangle$ atoms are expelled from the droplet region [13, 14, 33]. In addition, we find that the condensate 1D Thomas-Fermi radius in state $|\downarrow\rangle$ is $31 \mu\text{m}$, a value that is significantly lower than the expected radius of $57 \mu\text{m}$ for our parameters in the single component simulation with $\Omega \rightarrow 0$, i.e. with the BMF

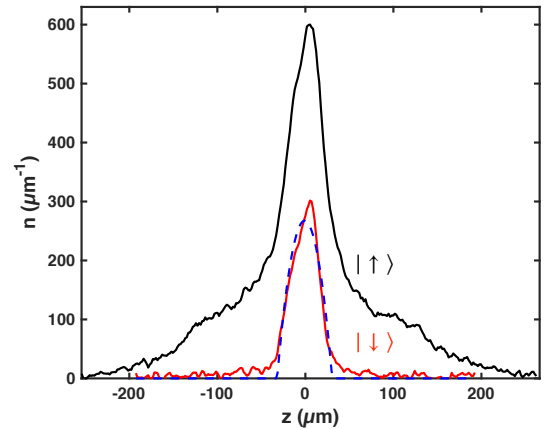


FIG. 3: Density profiles for $|\uparrow\rangle$ (black) and $|\downarrow\rangle$ (red) atoms after 75 ms of expansion at $\Omega = 0$. The blue dashed curve is a 1D Thomas-Fermi fit of the density profile in state $|\downarrow\rangle$.

energy density scaling with $n^{5/2}$. This difference indicates a significant role of transient MF effects in the expansion dynamics of the central region. Here, $|\uparrow\rangle$ atoms, which are more abundant than expected and which require some time to escape, create an excessive effective trapping for $|\downarrow\rangle$ atoms forcing their slower expansion.

In conclusion, we have studied both theoretically and experimentally, the BMF equation of state of a coherently-coupled two-component BEC in the asymmetric case at the special point (3) where the MF energy vanishes. The BMF energy density as a function of n interpolates between the usual $\propto n^{5/2}$ LHY form in the uncoupled limit to a qualitatively different behavior in the strong-coupling regime where one can introduce a hierarchy of effective BMF N -body interactions with $N = 2, 3, \dots$. We quantitatively verify our theoretical findings in an experiment where the BMF energy governs the condensate expansion and can thus be accurately measured. Our results open the path to the creation of coherently-coupled quantum droplets in which the two-body interaction (MF+BMF) is compensated by BMF three-body effects [22]. Interestingly, a coherent Rabi coupling helps to preserve the spin composition and thus prevents the system from dynamically drifting away from the point of vanishing mean field and thus facilitates direct measurements of the BMF equation of state.

We thank L. Tarruell for useful discussions. This research has been supported by CNRS, Ministère de l'Enseignement Supérieur et de la Recherche, Labex PALM, Région Ile-de-France in the framework of DIM Sirteq, Paris-Saclay in the framework of IQUPS, ANR Droplets (19-CE30-0003), Simons foundation (award number 563916: localization of waves). AR acknowledge financial support from Provincia Autonoma di Trento, the FISH project of the Istituto Nazionale di Fisica Nucleare, and the Italian MIUR under the PRIN2017 project

* Corresponding author: `thomas.bourdel@institutoptique.fr`

- [1] J. Armijo, Direct Observation of Quantum Phonon Fluctuations in a One-Dimensional Bose Gas, *Phys. Rev. Lett.* **108**, 225306 (2012).
- [2] T. Rentrop, A. Trautmann, F. A. Olivares, F. Jendrzejewski, A. Komnik, and M. K. Oberthaler, Observation of the Phononic Lamb Shift with a Synthetic Vacuum, *Phys. Rev. X* **6**, 041041 (2016).
- [3] J.-C. Jaskula, G. B. Partridge, M. Bonneau, R. Lopes, J. Ruaudel, D. Boiron, and C. I. Westbrook, Acoustic Analog to the Dynamical Casimir Effect in a Bose-Einstein Condensate, *Phys. Rev. Lett.* **109**, 220401 (2012).
- [4] J. Steinhauer, Observation of quantum Hawking radiation and its entanglement in an analogue black hole. *Nat. Phys.* **12**, 959 (2016).
- [5] R. Chang, Q. Bouton, H. Cayla, C. Qu, A. Aspect, C.I. Westbrook, and D. Clément, Momentum-Resolved Observation of Thermal and Quantum Depletion in a Bose Gas, *Phys. Rev. Lett.* **117**, 235303 (2016).
- [6] R. Lopes, C. Eigen, N. Navon, D. Clément, R.P. Smith, and Z. Hadzibabic, Quantum Depletion of a Homogeneous Bose-Einstein Condensate, *Phys. Rev. Lett.* **119**, 190404 (2017).
- [7] T. D. Lee, K. Huang, and C. N. Yang, Eigenvalues and Eigenfunctions of a Bose System of Hard Spheres and Its Low-Temperature Properties, *Phys. Rev.* **106**, 1135 (1957).
- [8] S. B. Papp, J. M. Pino, R. J. Wild, S. Ronen, C. E. Wieman, D. S. Jin, and E. A. Cornell, Bragg Spectroscopy of a Strongly Interacting ^{85}Rb Bose-Einstein Condensate, *Phys. Rev. Lett.* **101**, 135301 (2008).
- [9] N. Navon, S. Piatecki, K. Günter, B. Rem, T. C. Nguyen, F. Chevy, W. Krauth, and C. Salomon, Dynamics and Thermodynamics of the Low-Temperature Strongly Interacting Bose Gas, *Phys. Rev. Lett.* **107**, 135301 (2011).
- [10] I. Ferrier-Barbut, H. Kadau, M. Schmitt, M. Wenzel, and T. Pfau, Observation of Quantum Droplets in a Strongly Dipolar Bose Gas, *Phys. Rev. Lett.* **116**, 215301 (2016).
- [11] L. Chomaz, S. Baier, D. Petter, M. J. Mark, F. Wächtler, L. Santos, and F. Ferlaino, Quantum-Fluctuation-Driven Crossover from a Dilute Bose-Einstein Condensate to a Macrodroplet in a Dipolar Quantum Fluid, *Phys. Rev. X* **6**, 041039 (2016).
- [12] D.S. Petrov, Quantum mechanical stabilization of a collapsing Bose-Bose mixture, *Phys. Rev. Lett.* **115**, 155302 (2015).
- [13] R. Cabrera, L. Tanzi, J. Sanz, B. Naylor, P. Thomas, P. Cheiney, and L. Tarruell, Quantum liquid droplets in a mixture of Bose-Einstein condensates, *Science* **359**, 301 (2018).
- [14] G. Semeghini, G. Ferioli, L. Masi, C. Mazzinghi, L. Wolswijk, F. Minardi, M. Modugno, G. Modugno, M. Inguscio, and M. Fattori, Self-Bound Quantum Droplets of Atomic Mixtures in Free Space, *Phys. Rev. Lett.* **120**, 235301 (2018).
- [15] E. V. Goldstein and P. Meystre, Quasiparticle instabilities in multicomponent atomic condensates, *Phys. Rev. A* **55**, 2935 (1997).
- [16] M. R. Matthews, B. P. Anderson, P. C. Haljan, D. S. Hall, M. J. Holland, J. E. Williams, C. E. Wieman, and E. A. Cornell, Watching a Superfluid Untwist Itself: Recurrence of Rabi Oscillations in a Bose-Einstein Condensate, *Phys. Rev. Lett.* **83**, 3358 (1999).
- [17] J. Williams, R. Walser, J. Cooper, E. A. Cornell, and M. Holland, Excitation of a dipole topological state in a strongly coupled two-component Bose-Einstein condensate, *Phys. Rev. A* **61**, 033612 (2000).
- [18] T. Zibold, E. Nicklas, C. Gross, and M. K. Oberthaler, Classical Bifurcation at the Transition from Rabi to Josephson Dynamics, *Phys. Rev. Lett.* **105**, 204101 (2010).
- [19] E. Nicklas, H. Strobel, T. Zibold, C. Gross, B. A. Malomed, P. G. Kevrekidis, and M. K. Oberthaler, Rabi Flopping Induces Spatial Demixing Dynamics, *Phys. Rev. Lett.* **107**, 193001 (2011).
- [20] E. Nicklas, M. Karl, M. Höfer, A. Johnson, W. Muesel, H. Strobel, J. Tomkovic, T. Gasenzer, and M. K. Oberthaler, Observation of Scaling in the Dynamics of a Strongly Quenched Quantum Gas, *Phys. Rev. Lett.* **115**, 245301 (2015).
- [21] T. M. Hanna, E. Tiesinga, and P. S. Julienne, Creation and manipulation of Feshbach resonances with radiofrequency radiation, *New Journal of Physics* **12**, 083031 (2010).
- [22] D. S. Petrov, Three-Body Interacting Bosons in Free Space, *Phys. Rev. Lett.* **112**, 103201 (2014).
- [23] J. Sanz, A. Frölian, C. S. Chisholm, C. R. Cabrera, L. Tarruell, Interaction control and bright solitons in coherently-coupled Bose-Einstein condensates, arXiv:1912.06041
- [24] A. Farolfi, A. Zenesini, D. Trypogeorgos, C. Mordini, A. Gallemì, A. Roy, A. Recati, G. Lamporesi, G. Ferrari, Quantum-torque-induced breaking of magnetic domain walls in ultracold gases, arXiv:2011.04271
- [25] A. Cappellaro, F. Macri, G. Bertacco, and L. Salasnich, Equation of state and self-bound droplet in Rabi-coupled Bose mixtures, *Scientific Reports* **7**, 13358 (2017).
- [26] T.G. Skov, M.G. Skou, N.B. Jrgensen, J.J. Arlt, Observation of a Lee-Huang-Yang Fluid, arXiv:2011.02745.
- [27] M. Abad and A. Recati, A study of coherently coupled two-component Bose-Einstein condensates, *Eur. Phys. J D* **67**, 148 (2013).
- [28] A. Hammond, *et al.*, to be published.
- [29] See supplemental material.
- [30] E. Tiemann, P. Gersema, K.K. Voges, T. Hartmann, A. Zenesini, and S. Ospelkaus, Beyond Born-Oppenheimer approximation in ultracold atomic collisions, *Phys. Rev. Research* **2**, 013366 (2020).
- [31] X. Antoine and R. Duboscq, GPELab, a Matlab Toolbox to Solve Gross-Pitaevskii Equations II: Dynamics and Stochastic Simulations, *Computer Physics Communications* **193**, 95 (2015).
- [32] L. Lavoine and T. Bourdel, Beyond-mean-field crossover from one dimension to three dimensions in quantum droplets of binary mixtures, *Phys. Rev. A* **103**, 033312 (2021).
- [33] G. Ferioli, G. Semeghini, S. Terradas-Briansó, L. Masi, M. Fattori, and M. Modugno, Dynamical formation of quantum droplets in a ^{39}K mixture, *Phys. Rev. Research* **2**, 013269 (2020).
- [34] P. Cheiney, C. R. Cabrera, J. Sanz, B. Naylor, L. Tanzi,

and L. Tarruell, Bright Soliton to Quantum Droplet Transition in a Mixture of Bose-Einstein Condensates, *Phys. Rev. Lett.* **120**, 135301 (2018).

- [35] We have found that at low Rabi frequencies ($\Omega/2\pi \leq 7$ kHz), magnetic field noise around these frequencies transfers a small fraction of the atoms to state $|+\rangle$ during the condensate expansion (3% at $\Omega/2\pi = 6.9$ kHz, 4.5% at $\Omega/2\pi = 5.5$ kHz, 10% at $\Omega/2\pi = 3.9$ kHz, 12% at $\Omega/2\pi = 3.1$ kHz).
- [36] We have checked that for our parameters including the δ dependence of E_{BMF} leads to shifts of the minimal energy below 1%.
- [37] This averaging dominantly takes place at the single shot level during the expansion for the dominant 50 Hz, 100 Hz noise frequencies.
- [38] If all losses are solely attributed to three-body losses in state $|\downarrow\rangle$, taking into account the lower fraction of atoms in this states, our value corresponds to $K_{\downarrow\downarrow\downarrow} = 4 \times 10^{-26} \text{ cm}^6 \cdot \text{s}^{-1}$, which is ~ 7 times higher than previously measured values in thermal gases [14, 34]. This indicates that other collision channels are probably important.